

Supplementary Information

Confocal absorption spectral imaging of MoS₂: Optical transitions depending on the atomic thickness of intrinsic and chemically doped MoS₂

Krishna P. Dhakal,^{a,b} Dinh Loc Duong,^a Jubok Lee,^{a,b} Honggi Nam,^a Minsu Kim,^a Min Kan,^{a,c} Young Hee Lee^{a,b} and Jeongyong Kim^{a,b*}

^aCenter for Integrated Nanostructure Physics, Institute for Basic Science (IBS), Suwon 440-746, Korea.

^bDepartment of Energy Science, Sungkyunkwan University, Suwon 440-746, Korea.

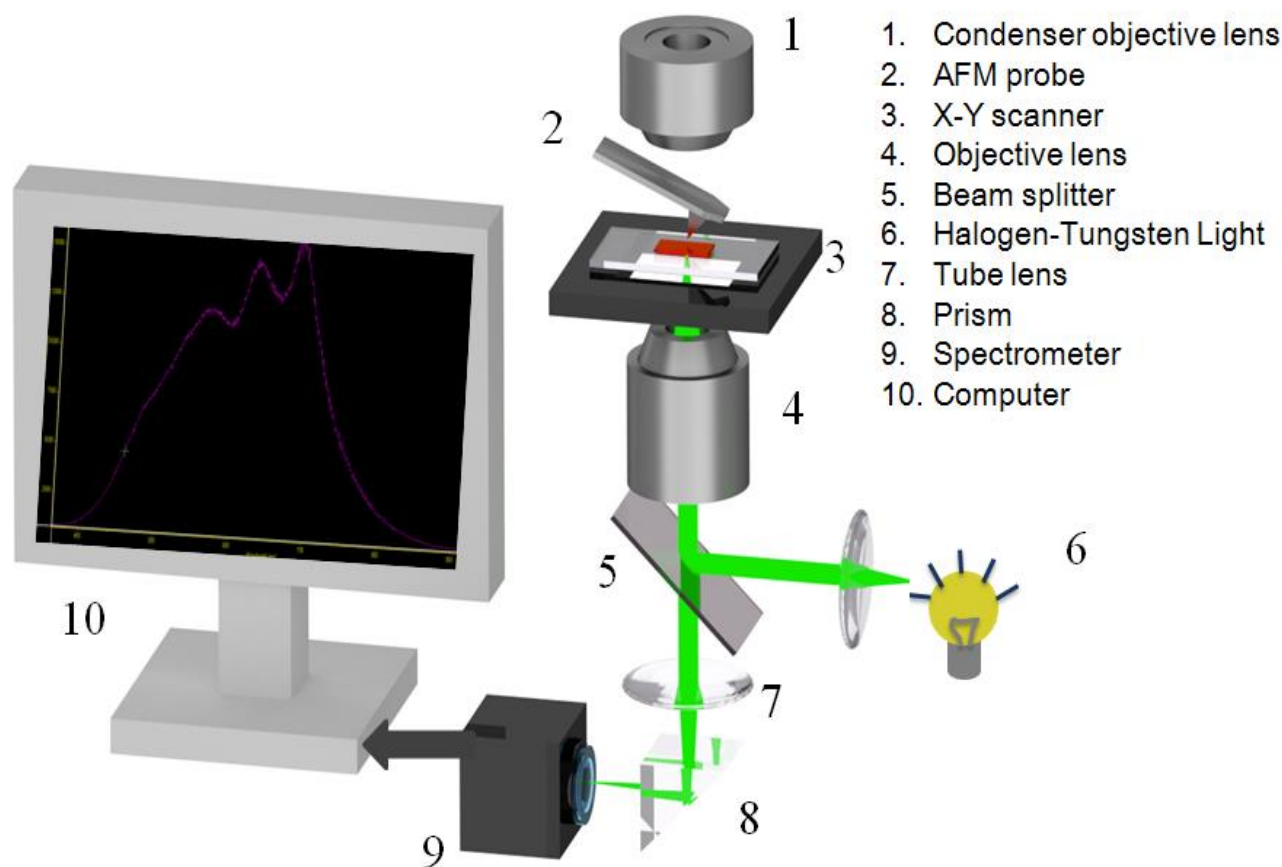
^cDepartment of Materials Science and Engineering, Peking University, Beijing 100871, China.

*Corresponding author. E-mail: j.kim@skku.edu, phone: +82-(0)31-299-4054 (O), Fax: +82-(0)31-299-4279

This Supplementary Information presents following contents:

- I. Schematic of the confocal absorption spectral mapping
- II. Identification of layer thickness using AFM and Raman spectral data
- III. Confocal absorption spectral imaging of the mono-, bi- and bulk MoS₂ (2nd set of data)
- IV. Schematic of n-type doping of the MoS₂ film using reduced BV and FT-IR results of intrinsic and chemically doped MoS₂ film
- V. Spectral decomposition of the PL peaks of intrinsic and chemically doped MoS₂
- VI. Comparison of absorption spectra with compensation of wavelength dispersion of the refractive index of the glass substrate

Schematic of the confocal absorption spectral mapping

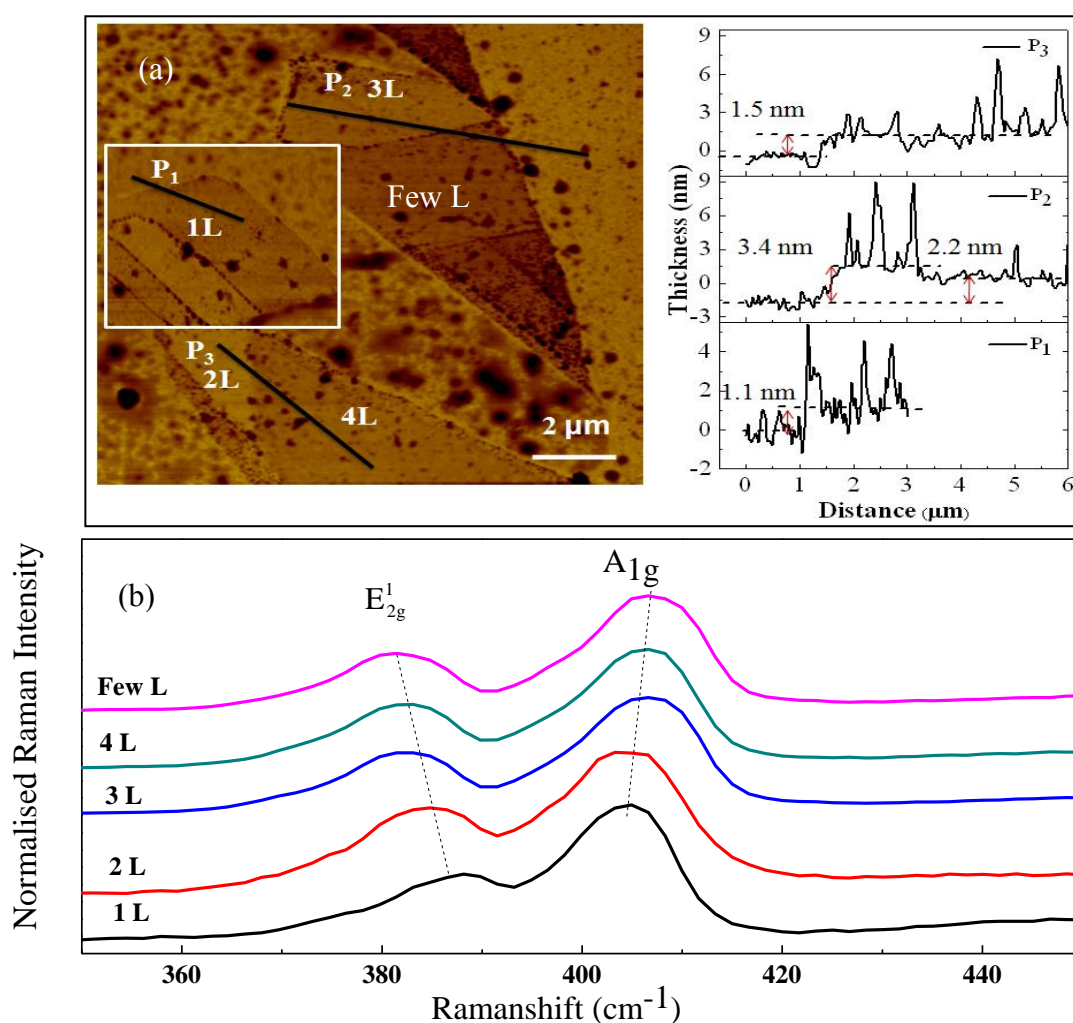


S1: Schematic of the AFM combined with confocal photoluminescence, Raman and absorption measurement systems in a backscattering geometry.

As shown in Fig. S1, confocal absorption spectral imaging was carried out using a lab-made laser confocal microscope system with a tungsten-halogen lamp acting as a broadband light source. By placing a confocal pinhole in front of the spectrometer, only light coming from a focal area of less than 1 μm in diameter was detected by the spectrometer. Once spectral mapping was completed, we used the background spectra obtained from the glass substrate to extract the absorption spectra from the sample. This approach meant that there was no need to focus the illuminating light on the sample as in differential reflectance spectroscopy.^{2,3} By combining an atomic force microscope (AFM) with this

system, we could obtain precise topographic information on the region of the sample from which the PL, Raman and absorption spectroscopic data were obtained, thus enabling us to observe the local spatial variations in the absorption properties with sub-micron resolution.¹ The spectral acquisition time at each pixel was relatively short (typically 20 ms for the absorption data presented), which is suitable for spectral mapping.

Identification of layer thickness using AFM and Raman spectral data



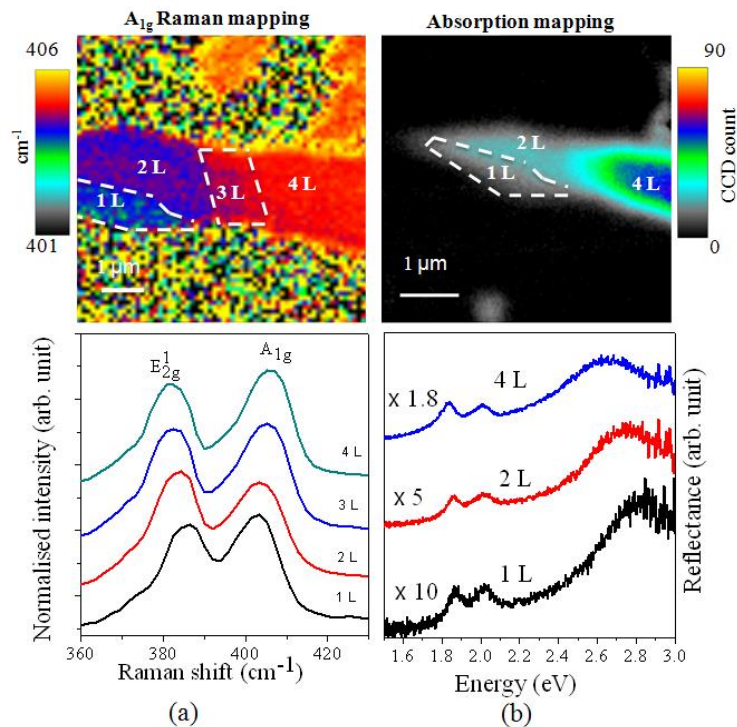
S2: (a) AFM images of the monolayer, bilayer and few-layer MoS₂ films. Line profiles from each of the regions are shown on the right. (b) Raman spectra recorded at each of the regions are in agreement with the layer thickness identified by AFM. A 514.5 nm excitation laser line was used for the Raman spectral imaging.

Table S1: Peak wavenumber and wavenumber difference between A_{1g} and E_{2g}^1 Raman bands of mono-, bi-, and few-layer MoS_2 . Excitation laser wavelength was 514.5 nm.

Number of layers	E_{2g}^1	A_{1g}	Wavenumber difference	Wavenumber difference ⁽⁴⁾
Mono layer	386.9	404.6	17.7	18.7
Bilayer	384.8	404.9	20.1	21.5
Trilayer	383.1	406.4	23.3	23.1
Quadruple layer	383.1	406.7	23.6	24.3

Confocal absorption spectral imaging of the mono-, bi- and bulk MoS_2 (2nd set of data)

Raman peak positions of MoS_2 samples with different numbers of layers using the 488 nm laser line are shown in Table S2. Confocal absorption measurements were then carried out on the same area. The variations in the optical transition values in Table S3 are very consistent with the 1st set of data provided in the main text.



S3: Raman characterizations of MoS_2 films using 488 nm laser excitation and confocal absorption spectral mapping of the same regions. (a) Raman mapping image (A_{1g} peak frequency) and averaged

Raman spectra obtained from 1L, 2L, 3L, 4L. (b) Absorption spectral mapping image of integrated absorption intensity and the averaged absorption spectra obtained from the layers. The Raman and absorption spectra are normalized by the respective multiplication factors and translated vertically for the easy comparison.

Table S2: Peak wavenumber and the wavenumber difference between A_{1g} and E_{2g}^1 Raman bands of mono-, bi- and few layers MoS_2 . Excitation laser wavelength is 488 nm.

Number of Layer	E_{2g}^1	A_{1g}	Wavenumber difference	Wavenumber difference ⁽⁵⁾
Mono layer	386.1	403.1	17.0	18.1
Bilayer	384.3	404.0	19.7	22.2
Trilayer	383.0	405.6	22.6	23.3
Quadra Layer	382.6	406.9	24.3	24.5

Table S3: Peak positions of absorption bands of the A exciton, B exciton and background (BG) bands. Spin-orbit coupling (SOC) strength and the observed shift in the difference between the A exciton peak position and BG peak are shown.

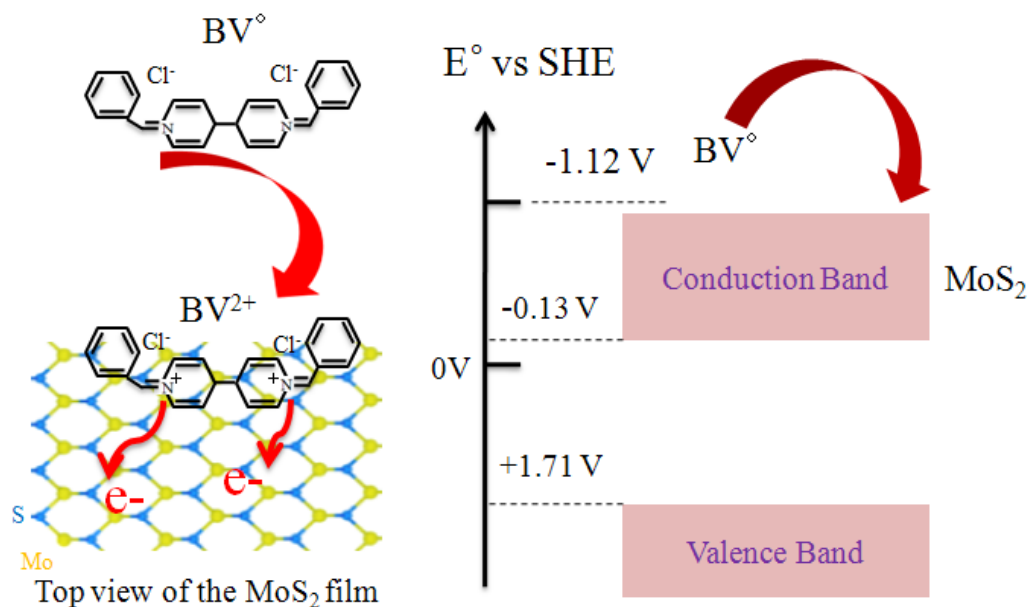
	Mono layer		Bilayer		Trilayer	Bulk	
	Set 1	Set 2	Set 1	Set 2	Set 1	Set 1	Set 2
A position	1.89	1.87	1.86	1.85	1.83	1.82	1.83
B position	2.03	2.02	2.02	2.01	2.01	2.01	2.01
BG ^a peak	2.84	2.83	2.73	2.72	2.63	2.61	2.63
BG shift	0	0	-0.11	-0.11	-0.21	-0.23	-0.20
SOC ^b (exp.)	0.14	0.15	0.16	0.16	0.18	0.19	0.18

EL ^c shift	0	0	-0.03	-0.02	-0.06	-0.07	-0.05
-----------------------	---	---	-------	-------	-------	-------	-------

a. Back ground, b. Spin-orbit coupling c. Exciton level

Schematic of n-type doping of the MoS₂ film using reduced BV and FT-IR results of intrinsic and chemically doped MoS₂ film

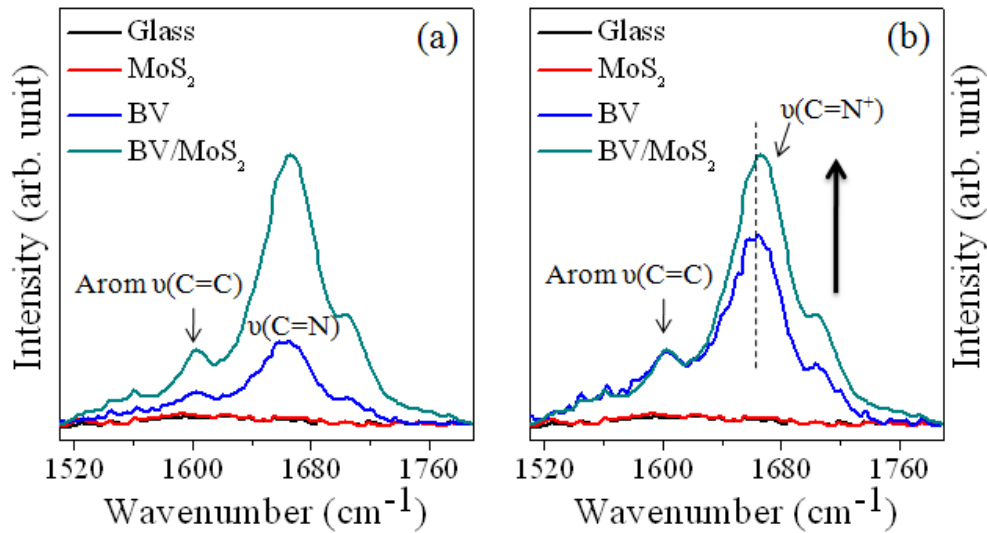
The mechanism of the solution based surface doping using the chemical 1,1'-dibenzyl-4,4'-bipyridinium dichloride (BV or BV^o) is shown in the schematic diagram, Figure S4. The principle of the chemical doping of MoS₂ using neutral BV label as BV^o in the Figure S4 is based on the redox reaction. The schematic in the Figure S4 (right panel) demonstrate much higher negative reduction potential of the BV than MoS₂ which clearly mean the possibility of the surface charge transfer from the BV molecules to the MoS₂ film to have n-type doping effect. As the surface charge transfer from the molecule BV to the MoS₂ takes place, BV converted into BV²⁺ from its original neutral charge state (BV^o) which is shown in the schematic S4 (left panel).



S4: Schematic of the structure of the dopant (BV^o), acceptor (MoS₂) and their relative reduction potential vs SHE (right panel). Data for the reduction potential are taken from the ref. [6] for BV and

ref. [7] for the MoS₂. The left panel of the schematic demonstrates the mechanism of the charge transfer from the BV molecules to the MoS₂ film as it is adsorbed on the surface of the MoS₂ film.

The evidence of the charge transfer from the BV to MoS₂ film is also observed from the IR spectra analysis of the BV film, on and off the few layer thick MoS₂ flake exfoliated on glass slide. We used the micro FTIR instrument (Hyperion 2000) to measure the IR spectra of the BV film from the glass substrate and from the MoS₂ flake. We found that IR spectra of BV enhanced on the MoS₂ film as shown in the Figure S5 (a). Aromatic stretching of the C=C bond at 1600 cm⁻¹ and C=N stretching in the 1650-1700 cm⁻¹ is observed from the BV film⁸⁻¹⁰ that was on the glass substrate while the signal from the BV on the MoS₂ was much higher. It is noted that MoS₂ and glass have no IR bands resonance with the IR band of the BV molecules in the spectral region selected in the study. We further normalized the IR bands of BV obtained from the glass surface and from the MoS₂ film at aromatic C=C vibration (1600 cm⁻¹) to remove the intensity enhancement factor due to aggregation of BV on the MoS₂ surface and analyze as shown in the Figure S5(b). We observed that IR band of the BV on the MoS₂ film showed relatively enhanced intensity and slightly up shifted nature of the C=N stretching in the wavenumber range 1650-1700 cm⁻¹. This effect is attributed as the conversion of the C=N bond to the C=N⁺ bond as suggested by the previous studies in which the IR band of C=N⁺ had shown as the enhanced absorbance with slightly up shifted peak positions than that of C=N vibration⁸⁻¹⁰. This result confirmed the successful charge transfer from the BV to MoS₂ film.

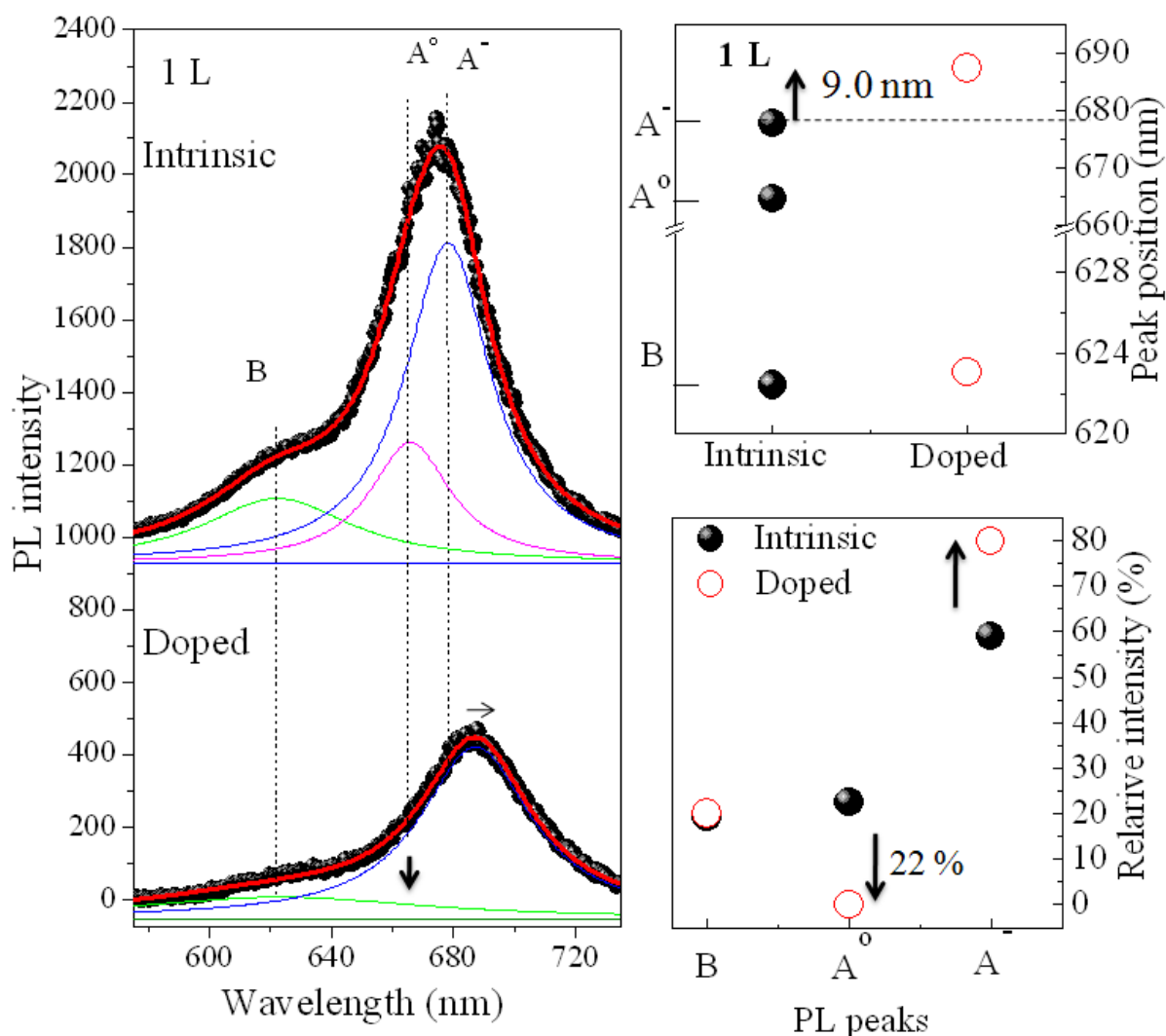


S5: FTIR spectra of the chemical dopant BV. (a) IR bands of the BV obtained from the glass substrate (blue curve) and that from the few layer thick MoS₂ film (green curve). (b) IR bands of BV normalized with the IR band of the arom (C=C) stretching vibration, showing the enhanced absorption intensity corresponding to the (C=N) stretching vibration.

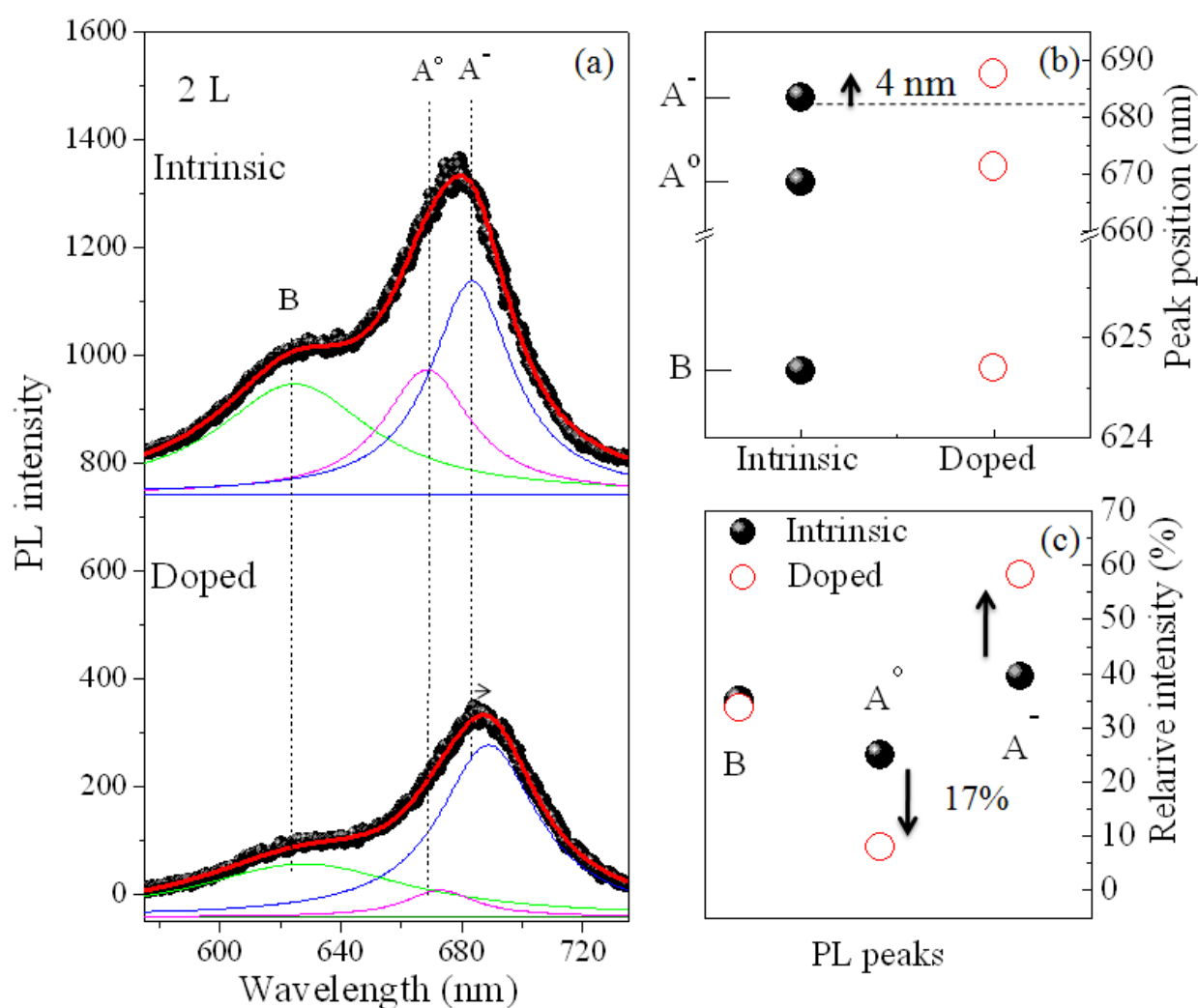
Spectral decomposition of the PL peaks of intrinsic and chemically doped MoS₂

The n-type chemical doping effect on the PL spectra of the different thicknesses MoS₂ films are analyzed by splitting the A exciton peak into two Lorentzian curve, neutral exciton A⁰ and negative trion A⁻. The effect of the chemical doping performed by the drop cast method on the area of various thicknesses MoS₂ film has been analyzed by means of decomposition of the neutral exciton (A⁰) and trion (A⁻) peaks. 1 L MoS₂ film showed the largest effect by n-type chemical doping by BV in which the neutral exciton completely quenched with enhancement of trion peak as shown in the Figure S6 (a-c). The Lorentzian fitting to the intrinsic and chemically doped n-type 1 L MoS₂ film is in agreement with the reduction of the neutral exciton and the increase and the redshift of the trion peak reported by the previously results.^{7,11}

We also split the A exciton peak for the 2L and 4L PL spectra and demonstrate in the Figure S7 and S8 respectively. The trend of the neutral exciton quenching and the increase and the red shift of the trion peak with increasing the atomic thickness is clear. These spectral behaviors is consistent with our observation of the quenching and the red shift to the PL peak position of the chemically n-type doped MoS₂ films. In addition the decreasing trend of these spectral modifications with increasing the thicknesses due to the chemical doping suggests that solution based chemical doping is mostly effective on the top layer of the MoS₂ films.

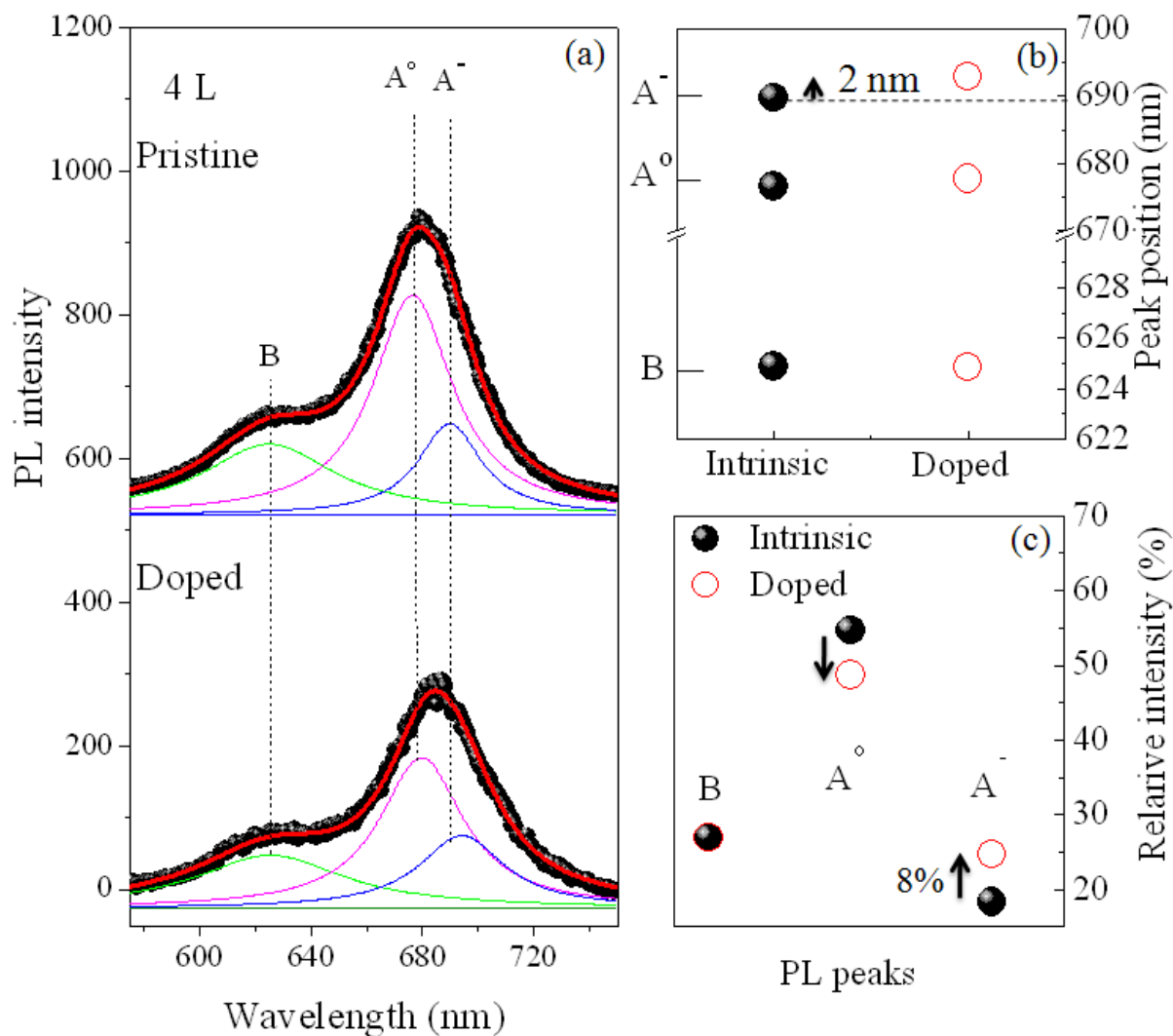


S6: (a) The Lorentzian fitting to the experimental data (black symbol) of the intrinsic and doped PL spectra from the 1 L MoS₂ film. Green, magenta and blue line represents the spectral behavior of the B, neutral exciton A[°] and trion A⁻ resonance peaks. (b) Peak positions of the B exciton, neutral exciton A[°] and trion A⁻. (c) Relative intensity variation of each peak before and after chemical doping.



S7: (a) The Lorentzian fitting to the experimental data (black symbol) of the intrinsic and doped PL spectra from the 2 L MoS₂ film. Green, magenta and blue line represents the spectral behavior of the

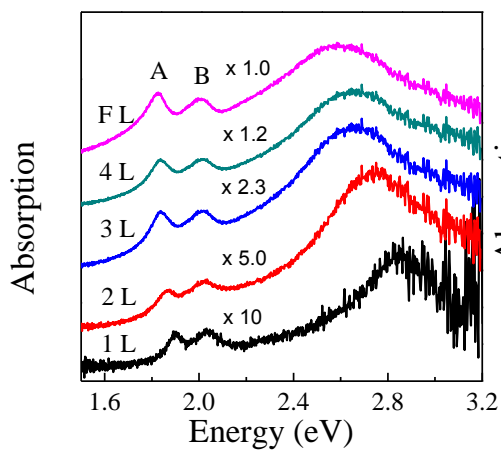
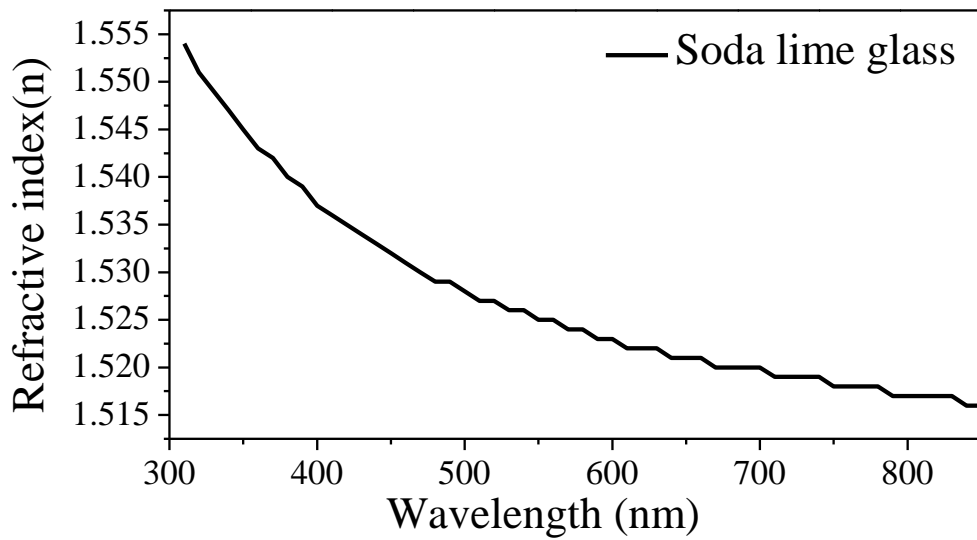
B, neutral exciton A° and trion A^{-} resonance peaks. (b) Peak positions of the B exciton, neutral exciton A° and trion A^{-} . (c) Relative intensity variation of each peak before and after chemical doping.



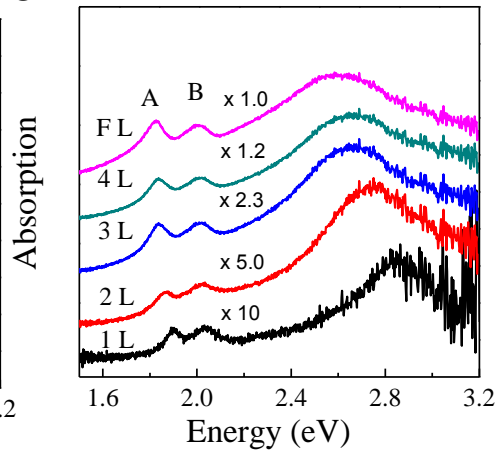
S8: (a) The Lorentzian fitting to the experimental data (black symbol) of the intrinsic and doped PL spectra from the 4 L MoS₂ film. Green, magenta and blue line represents the spectral behavior of the B,

neutral exciton A° and trion A^{-} resonance peaks. (b) Peak positions of the B exciton, neutral exciton A° and trion A^{-} . (c) Relative intensity variation of each peak before and after chemical doping.

Comparison of absorption spectra with compensation of wavelength dispersion of the refractive index of the glass substrate



Without considering the dispersion relation of the glass substrate



With considering the dispersion relation of the glass substrate

S9: (Upper panel) Dispersion of refractive index of soda lime glass with light wavelength [12]. Absorption spectra obtained with and without considering the wavelength dispersion of refractive index of the glass substrate in calculation of differential spectra using the equation (1) in the main text. The main characteristics of the absorption spectra for different layer number of MoS₂ films are virtually identical with consideration of index dispersion of the glass substrate.

Notes and references

1. H. Lee, J. H. Kim, K. P. Dhakal, J. W. Lee, J. S. Jung, J. Joo and J. Kim, *Appl. Phys. Lett.*, 2012, **101**, 113103.
2. W. Zhaoa, Z. Ghorannevisa, L. Chua, M. Toh, C. Klo, P-H. Tan and G. Eda, *ACS Nano*, 2013, **7**, 791-797.
3. K. F. Mak, K. He, J. Shan and T. F. Heinz, *Nat. Nanotechnol.*, 2012, **7**, 494-498.
4. C. Lee, H. Yan, L. E. Brus, T. F. Heinz, J. Hone and S. Ryu, *ACS Nano*, **2010**, **4**, 2695-2700.
5. H. Li, Q. Zhang, C. C. R. Yap, B. K. Tay, T. H. T. Edwin, A. Olivier and D. Baillargeat, *Adv. Funct. Mater.*, 2012, **22**, 1385-1390.
6. S. M Kim, J. H. Jang, K. K. Kim, H. K. Park, J. J. Bae, W. J. Yu, I. H. Lee, G. Kim, D. D. Loc, U. J. Kim, E.-H. Lee, H.-J. Shin, J.-Y. Choi and Y. H. Lee, *J. Am. Chem.Soc.*, 2009, **131**, 327-331.
7. S. Mouri, Y. Miyauchi and K. Matsuda, *Nano Lett.*, 2013, **13**, 5944-5948.
8. L. S. Lussier, C. Sandorfy, H. Le-Thanh and D. Vocelle, *J. phys. Chem.*, 1987, **91**, 2282-2287.
9. S. Liu, S. Gangopadhyay, G. Sreenivas, S.S. Ang and H. A. Naseem, *Phys. Rev. B*, 1997, **55**, 13020-13021.
10. V. A. Constantin, D. Bongard, L. Walder, *Eur. J.Org.Chem.*, 2012, **2012**, 913-921.
11. K. F. Mak, K. He, C. Lee, G. H. Lee, J. Hone, T. F. Heinz and J. Shan, *Nat. mater.*, 2013, **12**, 207-211.

12. M. Rubin, *Sol. Energ. Mater.*, 1985, **12**, 275-288.